

COMPUTER SIMULATION OF DOPPLER SPECTRA ASSOCIATED WITH MOVING SCATTERERS FOR DIFFERENT SOURCE CONFIGURATIONS AND ARBITRARY TRAJECTORIES.

Elazar Zonnenschein and Dan Censor
 Department of Electrical and Computer Engineering
 Ben Gurion University of the Negev
 Beer Sheva, 84105, Israel

Summary

A finite element method is developed for calculation of fields excited by focused radiators and scattered by moving particles, and the associated Doppler spectra. The algorithm was tested for known cases, e.g., the field along the axis of rectangular and circular aperture transducers. In all cases the algorithm generated data which adequately approximated solutions of simple canonical problems, and results published in the literature.

The known phenomenon of Doppler spectra broadening in the presence of disturbed flow is simulated here. It is shown that broadening and ripple are related to non-linear motion of particles within the sampling volume. Moreover, the results show that Doppler spectra broadening occurs around the Doppler central frequency and that the spectrum shape depends on the particle's motional characteristics and the sampling density. The results show that broadened spectra attributed to "flow reversal" are similar to spectra resulting from a disturbed flow within the sampling volume.

In Doppler systems it is necessary to derive the sign of the Doppler shift frequency, which depends on the particle's motion along the transducer's axis. This problem is usually solved by using a quadrature scheme. Accordingly, the received signal is split into two channels and multiplied by in phase and quadrature sinusoidal signals at the carrier frequency. It is shown that in the presence method, the quadrature is unnecessary. Consequently, time consuming calculations are obviated, and instead of sampling at the high frequency (RF), we deal directly with the Doppler shift frequencies.

The method described in this paper can be used as a research and design tool for focused radiators incorporating different aperture shapes, and for understanding the physical phenomena associated with field calculations and particle movements in different media. The high speed of the present algorithm facilitates its future incorporation into real time systems. Moreover, the algorithm is very flexible, hence relevant parameters can be varied over a wide range.

Introduction and preliminary considerations

This research has been undertaken in order to understand and explain the physical phenomena associated with Doppler spectra. Because of a lack of fundamental understanding, investigators often draw conclusions based on their intuition and experience. For example, doctors diagnose narrowing of blood vessels by observing Doppler spectra shapes without relating them to the physical processes occurring in the flow field and in the acoustical wave field. Basic processes simulations such as turbulent particle movement will enable investigators to make inferences based on an understanding of the physical phenomena occurring in the system. To this end, we need to calculate fields generated by different transducers, with particular emphasis on focused transducers.

With slight amendment, the present theory is applicable to scalar problems in other areas, for example, optics, hydrodynamics, radar and sonar.

In a review paper Luukkala¹ refers to the theory developed by O'Neil² for focused long aperture radiators. O'Neil stated that in special circumstances the Rayleigh integral can be used to describe the field solution for a focused transducer. Luukkala pointed out that O'Neil's evaluation is rigorous for an infinite rigid baffle only. In reality the shape and the properties of the transducer and the aperture, as well as those of the surrounding objects, affect the wave field. In principle, this must be properly incorporated into the boundary value problem at hand. However, because of the complexity of such a problem, the transducer is treated as a source distribution on some surface. It is well known that a planar distributed source in free space is equivalent to the same source (with half the amplitude, to be precise), distributed on a rigid baffle. Thus the treatment of the transducer as a planar aperture is an approximation which amounts to ignoring all the surrounding structure. This approximation still holds for non-planar sources, provided the radius of curvature everywhere is large compared to the wavelength³.

In the case of coherent radiation from several sources, the total field is the phasor sum of the fields contributed by the individual sources. This sum takes into account the relative phases of the fields and the summation expresses the averaged coherent field. In the case of many scatterers with statistically uncorrelated positions, this component of the field becomes vanishingly small. It follows that for this case the scattered field power from several scatterers is incoherent⁴ and therefore power spectrum amplitudes are additive.

For an ensemble of particles all having identical properties except for their uncorrelated positions, it is therefore justifiable to analyze the spectrum

produced by a single particle and use the amplitude spectrum (i.e. square root of the sum of the squares of the real and imaginary parts of the complex spectrum) as representative of the whole ensemble. While such considerations are strictly applicable to spatially infinite ensembles, they provide a good model for a finite but large collection of statistically uniformly distributed, small, noninteracting scatterers in a finite domain.

General discussions concerning Doppler- and, in particular, pulsed-Doppler systems are given for example by Baker, Forster and Daigle⁵, Wells⁶, and Fish⁷, with additional background material appearing in Hill⁸.

The Doppler effect⁹⁻¹¹ is used to measure the flow velocity by measuring the Doppler frequency shift produced by wave scattering from particles carried along by the flow. In a pulsed Doppler system, the transducer acts as a transmitter and receiver, on a time-sharing basis, and time gating of the received signal is implemented to record echoes from certain regions in space. The transmitter radiates energy at (angular) frequency ω_0 , corresponding to a frequency $f_0 = \omega_0 / 2\pi$ (henceforth, where no ambiguity might arise, the term frequency will be applied to ω and f indiscriminately). The ensuing wave scattered by a moving particle with velocity v will have a frequency

$$\omega = \omega_0 \left(1 - \frac{2v}{c} \cos\theta \right) \quad (1)$$

where θ is the angle subtended by the velocity and the transmitted wave propagation vector, and c is the wave propagation velocity in the medium, see Fig. 1. Formula (1), although sometimes referred to as the Doppler principle is, at best, a first order approximation in the Mach number v/c , based on plane wave notions, and ignores much of the physics of the system¹². This fact must be emphasized because beyond this approximation, one must take into account nonlinear effects. As far as these authors are aware, it is invariably assumed that the particle velocity is identical with the flow velocity, the Doppler effect is computed assuming that the particles are in motion but that the moving medium has no effect on the frequency shift. This amounts to an assumption that, as far as the Doppler effect is concerned, the medium around the moving particles is at rest¹². Moreover, all the Doppler techniques employed by researchers assume that if we compute the wave field at a position defined by a vector r and then substitute into the resulting expression the particle's equation of motion $r = r(t)$, a legitimate solution of the wave equation is obtained. This "quasi-static" approach has been shown to be conceptually inconsistent¹³. However, as long as equation (1) is used to obtain results of the zero order in v/c for the amplitude and the wave propagation vector, and of first order in v/c for the frequency, the solutions are valid. This approach is adopted here.

Pulsed Doppler systems usually incorporate focused transducers and the field generated is dependent on the propagation medium and the aperture function. We are mainly interested in the spectral effects introduced by specific flows, in the presence of a given transducer and its aperture. Therefore, in order to keep the main features and at the same time adhere to a simple model, it will be assumed that the medium is homogeneous, isotropic, linear, lossless, and time invariant.

The present algorithms afford a wide range of treatments for different apertures; however, we will limit our discussion to simple apertures, i.e. uniformly excited, focused transducers. In practice, focusing can be achieved in various ways: one method is to put a lens in front of the transducer aperture. Alternatively, the transducer can be constructed as a spherical surface, concave towards the wave transmission direction. In a third method, the transducer consists of an array of radiating elements and by suitably exciting the elements, each with its appropriate phase delay, one achieves focusing. In this paper we consider the last alternative, i.e., a plane transducer aperture excited at a constant amplitude across the transducer face, and a varying phase, such that the wavelets emanating from the various elements arrive in phase at certain point in space. Obviously this defines the point in question as the focus. Investigation of various transducer shapes and the associated fields has been undertaken by many authors; see for example, Marini and Rivenez¹⁴, Drost¹⁵, Gavrilov et al.¹⁶, Lucas and Muir¹⁷, Ocheltree and Frizzle¹⁹, and Yao, Zagzebski and Boote²⁰. In our finite element model we can achieve any desired transducer shape and arbitrary aperture functions. For example, we can, define without difficulty, complicated lenses, such as astigmatic lenses.

Finite element considerations

The use of the finite element method requires that a continuous system be converted into a discrete system model¹⁸. The discrete model is an approximation to the continuous one, this approximation becoming progressively better as the number of lattice points increases. In this way finer changes will also taken into account. The mathematical interpretation of this argument is expressed by the Nyquist theorem: The sampling process performed at an angular frequency 2ω recovers all continuous signal frequencies up to the frequency ω . Uniform lattice finite element methods facilitate the application of the Nyquist criterion to the spatial variations, thus providing an estimation for the quality of the approximation made. We note that finding the Nyquist frequency appropriate to a continuous system constitutes a class of problems by itself and, for simplicity, we will assume that our approximations are valid.

As the continuum is divided into elements, the basic unit retains its dimension, for example, a sampling process of a time interval will produce time elements. The elements are labeled by indices, and their size is determined by the number of elements N into which a given segment L is divided: Thus the i -th element will be represented by

$$\xi_i = \left(\frac{L}{N} \right)_i \quad i = 0, \dots, N-1 \quad (2)$$

We associate a magnitude $f(\xi_i)$ with each value ξ_i . Moreover we can associate values of a parameter ξ_i along a path $r(\xi_i)$ with a dependent variable $f(r)$. This concept applies to higher dimensionality as well, e.g., a three dimensional simple volume can be divided into element s , where the Cartesian coordinates are identified by three indices i, j, k . This facilitates the implementation of computational algorithms involving nested loop processes or parallel processing. Special treatment is necessary for specific categories of elements, for example consider the boundary lines of a given region, passing through elements, see Fig 2. The problem in this case consists of giving the appropriate weight to the sample $f(\xi_{ij})$. The approach adopted in the present computation method is to give the proper weight to the active part of the element through which the contour line passes. In this approach we identify the crossing points of the boundary contour and the element, and then we allocate a new weight to the active part of the element. The weight of the modified element is arbitrarily defined in terms of a weighted sum of the magnitudes of the element in question and its neighbors. In Fig. 2, A, B are the crossing points of the boundary contour and the element (i, j) , bounded by the coordinates $x_m, x_{m+1}, y_n, y_{n+1}$. The active part of the element is now defined as the relative area of the triangle ABC. The magnitude associated with this element will be calculated as follows: Consider the above discussed continuous function $f(r)$. Approximating $f(r)$ by the three leading terms of its Taylor expansion about the location r identified by A:

$$f(A) = f(x_m, y_n) + b\Delta y \frac{\partial f}{\partial y} \Big|_{(x_m, y_n)} + \frac{(b\Delta y)^2}{2!} \frac{\partial^2 f}{\partial y^2} \Big|_{(x_m, y_n)} \quad (3)$$

$$\text{The derivatives are approximated by the present method}^{18}, \text{ yielding } f(A) = \frac{(b+1)(b+2)}{2} f(x_m, y_n) - (b+1)(b+2) f(x_m, y_{n-1}) + \frac{b(b+1)}{2} f(x_m, y_{n-2}) \quad (4)$$

Similarly to (4), $f(B)$ follows by replacing b by a and y by x . Finally we can write

$$f(x_m, y_n) = \frac{f(A) + f(B)}{2} a\Delta x b\Delta y \quad (5)$$

For boundary line A', B', Fig 2, the active area is represented by the trapezoid A', B', C, D; $f(A')$, $f(B')$ can be calculated using the same procedures embodied in equations (3),(4). The case where the contour is like A'', B'' defines a triangular area that is subtracted from the element area. Now we can describe an arbitrary planar surface $f(x, y)=0$ bounded by a rectangle. To locate an element, define a coordinate system ξ, η , as described in Fig 1. In this system a point on the surface is located by the vector $\rho(\xi_m, \eta_n)$ whose length is

$$\rho_{mn} = \sqrt{\xi_m^2 + \eta_n^2} \quad \text{A trajectory which includes } N \text{ uniformly spaced sample points } i \text{ will be represented as}$$

$$x = x(t_i), \quad y = y(t_i), \quad z = z(t_i)$$

$$t_i = \left(\frac{t_{\text{end}} - t_{\text{begin}}}{N} \right)_i \quad i = 0, \dots, N-1 \quad (6)$$

where t_i is the dependent parameter. E.g., the parameter pertaining to the motion of a particle along a trajectory. In the coordinate system (Fig. 1), the vector \mathbf{R} connects the surface element x_{mn} on the aperture with a trajectory element denoted by the time sample t_i . For an aperture in the plane $z=0$

$$R_{i,m,n} = \sqrt{(x(t_i) - \xi_m)^2 + (y(t_i) - \eta_n)^2 + z(t_i)^2} \quad (7)$$

this length appears in the computation of the fields and the ensuing Doppler spectra.

Field computation

The radiation field from arbitrary apertures, and the associated Doppler spectrum caused by arbitrary particle motion in this field will be considered. The computation is based on the Rayleigh integral representation for the solution of the wave equation, using the finite element method. Newhouse et al.²², Censor et al.²³, computed the acoustical field in the focus plane by solving the Rayleigh integral

$$\Psi = e^{-i\omega_0 t} \int \frac{1}{R} e^{ikR} \Psi_a(\rho) dv(\rho) \quad R = |\mathbf{r} - \boldsymbol{\rho}| \quad (8)$$

where $\mathbf{R}, \boldsymbol{\rho}$ are described in Fig 1, $k=\omega/c$, and the volume differential dv is in this case replaced by a surface differential ds for a plane source. By using the Fraunhofer approximation, the acoustic field at the focus plane of long strip and circular aperture transducers has been derived. The time dependent particle location defines the temporal signal. The corresponding Doppler spectrum is given by its Fourier transformation. For other, arbitrary focal lengths, a closed form solution of the integral (8) does not exist, and equation (8) must be solved numerically. All parameters appearing in the Rayleigh integral are discretized. Because we are interested only in the relative magnitude of the field, the surface differential ds appearing in (8) will be assigned a unit value in a numerical integration. The field at any point on the particle trajectory (described by (6)) will be obtained as the phasor sum of all the contributions by the elements representing the aperture function. The element contribution is the excitation amplitude, $\Psi_a(\rho)$, multiplied by a spherical wave emitted from that element and measured at the particle location. The focus, by definition, is a point where all the wavelets arrive at the same phase. Hence we define a new position vector r_f

$$\text{whose magnitude } r_f \text{ is (see Fig 1)} \quad r_f = \sqrt{(\xi_m^2 + \eta_n^2 + F^2)} \quad (9)$$

where F is the focus length measured along the optical axis from $\xi=0, \eta=0$ on the aperture to the focus. We can now compute the field on the trajectory as a function of the descretized time t_i according to

$$\Psi(x_i, y_i, z_i, t_i) = e^{-i\omega_0 t_i} \sum_m \sum_n \frac{1}{R_i} e^{ik(R_i - r_f)} \Psi_a(\rho) ; |\boldsymbol{\rho}| = \sqrt{\xi_m^2 + \eta_n^2} \quad (10)$$

where x_i etc. stands for $x(t_i)$. Note that the field is a complex quantity,

however the graphical results depict the field intensity $\sqrt{\Psi \Psi^*}$ which is real. This graphic representation emphasizes the field envelope, the RF oscillations within this envelope is not displayed.

Doppler spectrum calculations

Essentially, we are interested in identifying various flow characteristics. Some of these features are related to the Doppler spectrum produced by scattering of waves by particles moving with the flow in question. The Doppler spectrum is obtained by applying the Fourier transform to the time signal associated with the relevant scattering process. More specifically, we are interested here in Doppler spectra produced in pulsed Doppler ultrasound systems. In such systems the signal detection and the calculation of Doppler spectra are intimately related to the time gating process involved. Therefore it is important to discuss the signal processing in these systems. The discussion below is simplified but it retains the important characteristics of the general problem. In the pulsed Doppler system, the transducer acts as transmitter and receiver on a time sharing basis. In a simplified manner, the transmitted signal can be described by:

$$\cos(\alpha\omega_0 t) \cos(\alpha\Omega t) \quad (11)$$

where $\alpha=1$, i.e., a carrier wave $\cos(\omega_0 t)$ modulated by an envelope $\cos(\Omega t)$, thus producing a pulse train at a pulse repetition (angular) frequency Ω . This signal is composed of frequencies $\pm\alpha\omega_0 \pm\alpha\Omega$. The echo is given by a Doppler frequency shifted signal similar to (11), where now $\alpha=(1-2v_z/c)$, v_z being the velocity in the z -direction. At the receiver, the signal is downshifted by ω_0 and gated at frequency Ω . This is tantamount to modulation procedures adding frequencies ω_0 and Ω . Thus at the receiver the spectrum includes $\pm(\alpha\pm 1)\omega_0 \pm(\alpha\pm 1)\Omega$. Low frequency components include $\pm(2v_z/c)\omega_0 \pm(1\pm 2v_z/c)\Omega$. The gating frequency Ω is sufficiently high to be low pass filtered out, leaving $\pm(2v_z/c)\omega_0 \pm(2v_z/c)\Omega$. Finally, because $\omega_0 \gg \Omega$, we practically obtain at the receiver's output the Doppler shift frequencies $\pm(2v_z/c)\omega_0$. It must be emphasized that the signal processing is not capable of discriminating between $+\omega_0 2v_z/c$ and $-\omega_0 2v_z/c$ so that we cannot determine the correct direction of movement (from or towards the transducer). In practical systems this problem is solved by using a quadrature device which separates the received signal into two channels multiplied by $\cos(\omega_0 t)$ and $\sin(\omega_0 t)$ respectively, and by comparing the phases of the output channels the flow

direction is determined⁸⁻⁹. In this way, the downshifted Doppler spectrum becomes $f(\omega - \omega_0)$.

For a long strip aperture transducer and a particle moving in x - z plane, the field dependency on x is given²² by $\text{sinc}(\beta) = \text{sinc}(\beta)/\beta$, where $\beta \approx x$. For this case, we get a spectrum with a triangular shape. Doppler frequencies on the triangle sides²² will be

$$\omega_{\text{low}} = \omega_0 \left(-\frac{2v_z}{c} + \frac{v_x}{c} \frac{W}{F} \right); \quad \omega_{\text{high}} = \omega_0 \left(-\frac{2v_z}{c} + \frac{v_x}{c} \frac{W}{F} \right) \quad (12)$$

Note that (12) applies within the Fraunhofer approximation for the far field and for a long strip transducer only. For other apertures and arbitrary motion trajectories analytic results are not available, therefore it is necessary to compute the field and the associated Doppler spectrum numerically. To compute the Doppler time signal Φ_i at the receiver output, the particle is considered to be a source. The output signal is the phasor sum of the signals arriving at the various receiver's elements

$$\Phi_i = \Phi(t_i) = \sum_m \sum_{n'} \Psi(x(t_i), y(t_i), z(t_i)) \Psi_a(\rho) \frac{1}{R_i} e^{ik(R_i - r_f)} \quad (13)$$

The Doppler spectrum is obtained by subjecting Φ_i to a fast Fourier transform (FFT). In (13) Ψ_r, k, r_f, R_i play the same role as in (7), (9) for the transmitter, now applying to the parameters associated with the receiver aperture; Ψ is already computed in (10). When the transmitter and receiver use the same aperture then the Doppler time signal computation reduces to

$$\Phi_i = \left(\sum_m \sum_{n'} \frac{1}{R_i} e^{ik(R_i - r_f)} \Psi_a(\rho) \right)^2 \quad (14)$$

It should be noticed that in (10), $e^{i\omega_0 t}$ appears in the field computation as a common factor. Therefore, in the present method there is no need to use the quadrature method mentioned above. This factor can be suppressed, amounting to a downshifting of the spectrum by ω_0 . Assume a

transmission signal $e^{-i\omega_0 t}$ which is represented in the spectrum by a frequency $+\omega_0$. A particle is moving according to $z=vt$. According to the Doppler effect,

the received signal will be $e^{-i\omega_0 t \left(1 - \frac{2v}{c}\right)}$ which is represented in the spectrum by a frequency $\omega_0(1-2v/c)$. In the detection process the signal is

shifted by ω_0 and we get the signal $e^{i\omega_0 t \frac{2v}{c}}$ which is represented in the spectrum by a frequency $-\omega_0(2v/c)$. On the other hand, for motion $z=-vt$ we obtain the downshifted signal at a frequency $+\omega_0(2v/c)$. It is clear that the spectrum is automatically dependent on the sign of the velocity. The parameter $\omega_0 t$ must be positive in order that the spectrum frequency location will be correct. Because the transmission frequency is always positive, it is necessary to ensure that $t \geq 0$. This is the same as saying that the Green function

$e^{ikR - i\omega_0 t/R}$, which describes the spherical wave emanated from the aperture element, is always causal. In a discrete algorithm, the fact that we can suppress the factor $e^{-i\omega_0 t}$ and automatically achieve the same effect produced by the quadrature arrangement is a great advantage, because the signal without the factor $e^{-i\omega_0 t}$ does not contain the fast changes of the carrier wave. Consequently there is no need to maintain an extremely high sampling rate (dictated by the high frequency of the signal $e^{-i\omega_0 t}$) and store the large number of samples prescribed by this high sampling rate.

Computation quantification

The number of computations in the present algorithm depends on several factors: The aperture function (transmitter, receiver), the trajectory of motion, and the FFT procedure. We define the transducer lattice as containing $m \times n$ elements. Assuming the time spans N samples, which is also the number of samples appearing in the FFT, then, the total number of operations pertaining to the field computations is $m \times n \times N \times 67$. This number does not take into account mathematical operations introduced by boundary corrections (usually this number is very small compared to $m \times n$). The number of Doppler time signal computations involved in solving (13) when the receiver is different from the transmitter is given by $(m \times n \times N \times 67)^2$, i.e., the square. When the transmitter and receiver aperture are identical then we get instead only $2(m \times n \times N \times 67)$. The number of Doppler spectrum computations will include the above number of Doppler time signal operations and in addition the number of operations associated with the FFT algorithm, given by $N \log_2 N$.

Results and discussion

The method was successfully tested for many results available from the literature. Here one example is demonstrated, that of a long strip transducer. The long strip aperture should be made long in one direction, say the y direction. Actually we did not take a long aperture, instead we took one element only in the y direction. The proper long strip aperture possesses a cylindrical symmetry with respect to the y direction, and in the far field its

distance dependence is of the kind $e^{ikR - i\omega_0 t} / \sqrt{R}$, where R is perpendicular to the y direction. The present configuration clearly is not a long strip transducer proper. Instead, it has a spherical symmetry with respect to each

element along the line $y=0$, with distance dependence $e^{ikR - i\omega_0 t} / R$. However, in the $y=0$ plane, the present reduced configuration possesses the same angular properties as the long strip transducer. It is noted that in the presently used Fraunhofer approximation the distance parameter is not taken into account when we calculate the spectrum. We choose a particle trajectory in the x - z plane symmetrical with respect to the focus. The simulation involved a line of 100 elements arranged in the $y=0$ plane along the x direction. The transducer size was $W=1$ cm; particle velocity in the x direction is $v_x=20$ cm/sec; the focus length is $F=2$ cm; the particle trajectory was sampled at 1024 points which is also the number of the FFT points; the transmission (RF) frequency 3MHz; the wave velocity in the medium is $c=1570$ m/sec; the particle equation of motion is given by $x(t) = x_0 + v_x t$, where $x_0 = -1$ cm and t changes between 0 to 0.1 sec. Obviously, the transducer and focus lengths are not compatible with the Fraunhofer far field approximation, so we must compare the results with the analytical formulas²²

$$\text{sinc}\left(\frac{\omega_0 W \sin \phi}{2c}\right); \quad \sin \phi = \frac{x(t)}{\sqrt{x(t)^2 + F^2}} \quad (15)$$

For small angles ϕ , we get $\sin \phi \approx \phi$, reducing (15) to the Fraunhofer approximation. The simulation results for the field intensity, i.e. the absolute value of the field, are displayed in Fig 3. The discrepancy compared to (15) is within 1%. We also simulated disturbed flow in a sample volume. This simulation demonstrated Doppler spectrum broadening caused by disturbed, or unsteady flow. This subject is important in medical diagnosis of the cardiovascular system, for example, blood flow in the carotid artery with various degrees of obstruction. This subject is described with more detail elsewhere²⁵. The disturbed flow is represented here by the particle's equation of motion

$$\begin{aligned} x(t) &= x_0 + v_x t + X \sin(\Omega t + \psi_x) \\ y(t) &= y_0 + v_y t + Y \sin(\Omega t + \psi_y) \\ z(t) &= z_0 + v_z t + Z \sin(\Omega t + \psi_z) \end{aligned} \quad (16)$$

We choose a simple harmonic movement to represent a disturbed flow. We shall examine the received Doppler spectrum for various angles of transmission. In order to examine the simple harmonic movement, we choose a path which is perpendicular to the harmonic vibration. In this case we keep the speed constant, i.e., $v = \sqrt{v_x^2 + v_y^2}$. We chose $v=0.4$ m/sec, $RF=3$ MHz, propagation velocity $c=1570$ m/sec, time interval 0.02 sec, the particle trajectory is symmetrical with respect to the focus. The field and the associated Doppler spectrum will be computed at 512 points. The harmonic movement described by (16) is simplified by setting ψ_x, ψ_z to zero and

setting $\Omega=200\pi$. The harmonic movement amplitude $U = \sqrt{X^2 + Z^2}$ was varied. For the case $U=0.1$ mm the results are described in Fig. 4, for $\theta=150^\circ$, and in Fig. 5 for $\theta=120^\circ$. In order to examine the spectrum broadening, two curves are displayed: The broken line corresponds to $U=0$, i.e., laminar flow. The solid line describes the harmonic flow (disturbed flow) for several transmission and receiving angles (see Fig 1). It can be seen that for various aspect angles the spectrum broadening is different. The maximum effect occurs when the harmonic vibration is along the z axis. These results are significant in view of the findings reported by Zwibel²⁶, who stated that Doppler spectra broadening indicates "reversal flow", i.e., spectral broadening is caused by velocity components opposite to the expected direction of the flow. Our results demonstrate that spectrum broadening will occur even when such reversal flow does not take place, provided the frequency modulation introduced by the harmonic, or disturbed, motion is sufficiently strong (i.e., is associated with a large index of modulation). Sometimes there are indeed physio-pathological cases in which reversal flow (part of the flow is in the reverse direction) occurs, accompanied by a broadened Doppler spectrum. Our results demonstrate the importance of distinguishing between the various mechanisms causing broadening.

References

1. M. Luukkala and A. Penttinen, "The impulse response and pressure near-field of a curved ultrasonic radiator," *J. Phys. D: Appl. Phys.*, **9**, 1547-1557, 1976.
2. H. T. O'Neil, "Theory of focusing radiators," *J. Acoust. Soc. Am.*, **21**, 516-526, 1949.
3. G. S. Kino, *Acoustic waves*, New Jersey: Prentice-Hall, 1987.
4. G. Yu, V. L. Newhouse and D. Censor, "On coherent radiation scattered by random ensembles", *J. of Sound and Vibration*, **122**, 399-412, 1988.
5. D. W. Baker, F. K. Forster and R. E. Daigle, "Doppler principles and techniques", in *Ultrasound: Its Applications in Medicine and Biology*, F.J. Fry Ed. New York: Elsevier, 161-287, 1978.
6. N. T. Wells, *Biomedical Ultrasonics*, Academic Press, 1977.
7. P. J. Fish, "Doppler methods", in *Physical Principles of Medical Ultrasonics*, C. R. Hill Ed. New York: Wiley, 338-376, 1986.
8. C. R. Hill, ed., *Physical Principles of Medical Ultrasonics*, C. R. Hill Ed. Wiley, 1986.
9. C. Doppler, "Über das farbige Licht der Dopplesterne und einiger anderer Gestirne des Himmels", *Abhandlungen der Königlich böhmischen Gesellschaft der Wissenschaften*, **5**, Folge 2, 465-482, 1843.
10. T. P. Gill, *The Doppler Effect: An Introduction to the theory of the effect*, Academic, 1965.
11. K. Toman, "Christian Doppler and the Doppler effect" *Eos.*, **65**, 1193 - 1194, 1984.
12. D. Censor, "Acoustical Doppler effect - is it a valid method?", *J. of the Acoustical Soc. Am.*, **83**, 1223-1230, 1988.
13. D. Censor, "Theory of the Doppler effect - fact, fiction and approximation", *Radio Science*, **19**, 1027-1040, 1984.
14. J. Marini and J. Rivenez, "Acoustical fields from rectangular ultrasonic transducers for non-destructive testing and medical diagnosis", *Ultrasonics*, 251-256, 1974.
15. C. J. Drost, "Near and farfield of strip-shaped acoustic radiators", *J. Acoust. Soc. Am.*, **65**, 565-572, 1979.
16. L. R. Gavrilov, V. N. Dmitriev, and L. V. Solontsova, "Use of ultrasonic receivers for remote measurements in biological tissues", *J. Acoust. Soc. Am.*, **83**, 1167-1178, 1988.
17. B. G. Lucas and T. G. Muir, "Field of a finite-amplitude focusing source", *J. Acoust. Soc. Am.*, **74**, 1522-1528, 1983.
18. D. S. Burnett, *Finite element analysis*, Addison-Wesley, 1987. International student edition, McGraw-Hill, 1979.
19. K. B. Ocheltree, and L. A. Frizzel, "Sound field calculation for rectangular sources", *IEEE Trans. on Ultrasonics, Ferroelectrics and Frequency Control*, **36**, 242-248, 1988.
20. L. X. Yao, J. A. Zagzebski, and E. J. Boote, "A fast algorithm to calculate ultrasound pressure fields from single-element transducers", *IEEE Trans. on Ultrasonics, Ferroelectrics and Frequency Control*, **36**, 446-451, 1989.
21. M. Born, E. Wolf, *Electromagnetic Theory of Propagation, Interference and Diffraction of Light*, Pergamon Press, 1965.
22. V. L. Newhouse, D. Censor, T. Vontz, J. A. Cisneros, and B. B. Goldberg, "Ultrasound Doppler probing of flows transverse with respect to beam axis", *IEEE Trans. on Biomed. Eng.*, **24**, 779-789, 1987.
23. D. Censor, V. L. Newhouse, T. Vontz and H. V. Ortega, "Theory of ultrasound Doppler-spectra velocimetry for arbitrary beam and flow configurations", *IEEE Trans. on Biomed. Eng.*, **35**, 740-751, 1988.
24. E. L. Madsen, M. M. Goodsit, J. A. Zagzebski, "Continuous wave generated by focused radiators", *J. Acous. Soc. Am.*, **70**, 1508-1517, 1981.
25. D. Censor and E. Zonnenschein, "Computer simulation of Doppler spectra associated with normal and unsteady flows in carotid sonography", In process.
26. W. J. Zwiebel, "Spectrum analysis in carotid sonography", *Ultrasound in Med. & Biol.*, **13**, 625-636, 1987.

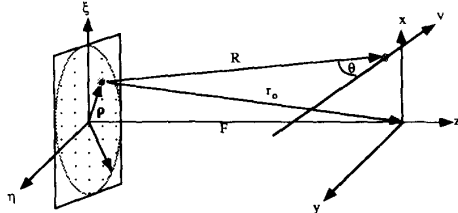


Fig. 1: Basic geometry for a pulsed Doppler system. System coordinates for shaped focused transducer associated with particle trajectory.

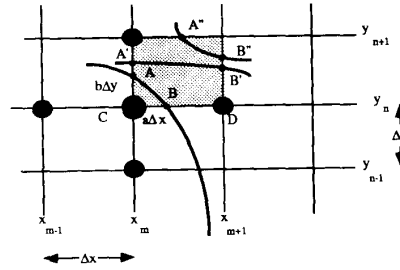


Fig. 2: Sketch of curved aperture in elements plane, showing the crossing points A, B and the boundary elements.

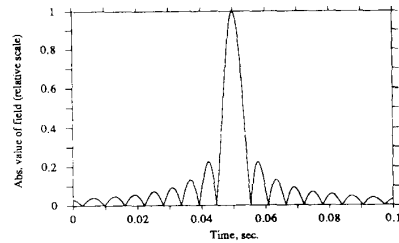


Fig. 3: Simulation result for absolute of the field measured in the focal plane of a strip transducer (see text for parameters and further comments).

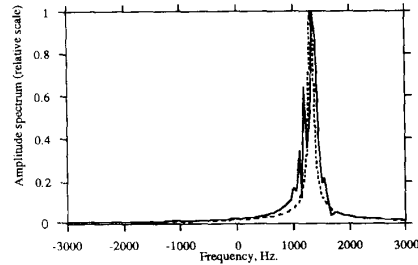


Fig. 4: Aspect angle 150⁰ (30⁰ angle with flow towards the transducer). Spectrum due to steady flow (dotted line) and broadening due to perpendicular unsteady flow component U=0.1mm.

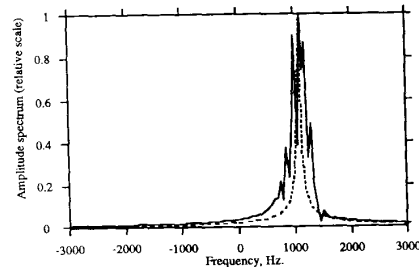


Fig. 5: Aspect angle 120⁰ (60⁰ angle with flow towards the transducer). Spectrum due to steady flow (dotted line) and broadening due to perpendicular unsteady flow component U=0.1mm. See text for details